PANIC4K Detector non-linearity correction data

PANIC4K

Prepared by	Bernhard Dorner José Miguel Ibáñez Mengual	Courtesy of CAHA Instituto de Astrofísica de Andalucía
Revised by	PANIC team	

Code: **PANIC4K-DET-TN-02**
Issue/Ver.: 2.0
Date: **08.04.2025**
No. of pages: 25

Document Change Log

Version	Date	Chapters affected	Comments
Issue 1.0 draft0	08.03.2024	All	Initial draft
Issue 2.0	08.04.2025	All	Update of calibration and verification with new reset settings

List of acronyms and abbreviations

AIV	Assembly, Integration and Verification
CAHA	Centro Astronómico Hispano en Andalucía
CDS	Correlated Double Sampling
IAA	Instituto de Astrofísica de Andalucía
GEIRS	**GE**neric **I**nfra**R**ed Detectors **S**oftware
MPIA	Max-Planck-Institut für Astronomie
NLC	Non-Linearity Correction
OT	Observing Tool
PANIC	**PA**noramic **N**ear **I**nfrared camera for **C**alar Alto
PAPI	**PA**NIC **PI**peline
QE	Quantum Efficiency

List of supporting documents

The following documents provide additional information about topics addressed in this document. They are referenced as RDx in the text:

RD Nr.	Identifier	Title	Issue	Date
RD 1	PANIC4K-DET-TR-01	PANIC4K detector characterization	1	30.05.2025
RD 2	PANIC4K-DET-TN-03	Electronic CDS offset	1	09.04.2025
RD 3	NTN-2013-004	Description of the NIRSpec linearity correction reference files	1.0	01.11.2013
RD 4	PANIC-SW-TN-04	PANIC FITS headers		
RD 5	PANIC-SW-DCS-01	Generic Infrared Software – Installation and User's Manual		

Contents

1 INTRODUCTION AND SCOPE

1.1 General

The new PANIC detector consists of one single Teledyne HAWAII-4RG array, replacing the old four Teledyne HAWAII-2RG detectors assembled in a 2x2 mosaic. It covers the instrument field of view with a sampling of 4096x4096 pixels.
This document describes the correction of the non-linear response of the new H4RG detector.

1.2 Contents

The document is structured into parts covering the effect of non-linear response, the calibration data creation, verification of the calibration, and the reference file format.

2 NATURE OF THE PROBLEM

HAWAII-4RG near-IR detectors exhibit an inherent non-linear response. It is caused by the change of the applied reverse bias voltage due to the accumulation of generated charge. The effect increases with signal levels, so that the measured signal deviates stronger from the incident photon number at higher levels, and eventually levels out when the pixel well reaches saturation.
The common approach is to extrapolate the linear signal $S_l(t)$ from measurements with low values, and apply a correction function of the measured data $S(t)$ to obtain the linear value:

$$S_l(t) = P(S(t)) \cdot S(t) \tag{1}$$

as long as $S(t)$ is below a maximum limit $S_{\max}$.

3 DATA

The effect was analyzed with flat-field images from the procedure DET_FLAT_4.6 as run from 2025/04/01 (Table 1). It comprises two sequences of images with rising integration time t from minimal (2.90s) to $t_{max} = 221\ s$.

Table 1: Procedures for flatfield data

Cycle	Name	Vers.	Date	Content	GEIRS and pattern
12	DET_FLAT	4.6	01/04/2025	Series of flatfields	r807M-76 (Feb 3 2025, 16:28:17)

The average saturation ($S \approx 47{,}000\ ADU$) was set to occur at $140s$. The exposure time span was sampled with a 2.9 s interval between 2.90 s and 29 s (10 points), and ~6 s in the range 35–221 s (36 points), having in total series of 46 points. The number of exposures was adjusted such that a total number of ~250,000 ADU was collected to keep the shot noise at about 0.2%.
The series was arranged in an even/odd order up the ramp, first with the exposures number 1, 3, 5, ..., then 2, 4, 6 etc. This allows to check for drifts in the light source which otherwise would impact the correction.

Besides, in between each calibration measurement, a reference exposure was taken with 35 s integration time and 10 repetitions. These are used to monitor the source and measurement stability, and correct the data according to relative signal level during the measurement duration. The interval corresponds to about 20—30 minutes.

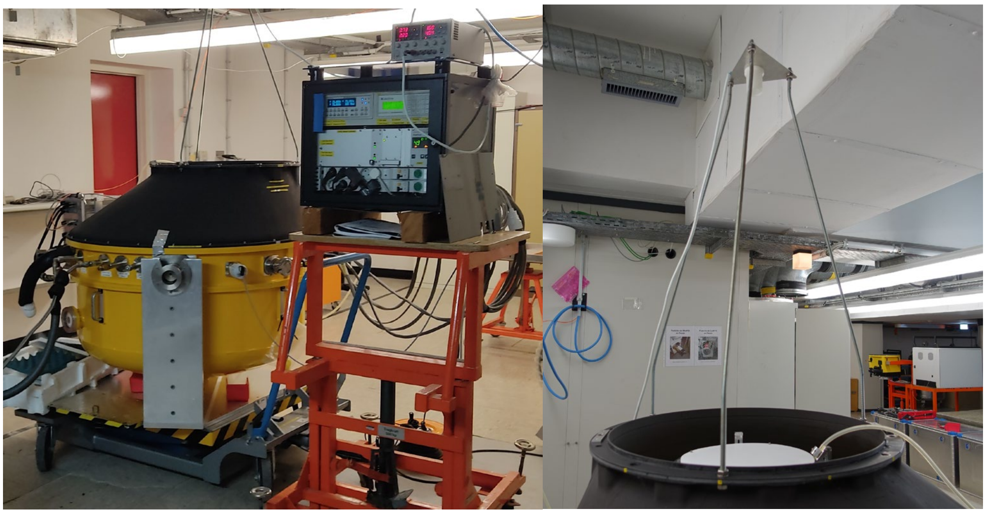

Figure 1: Lamp lab setup for the flatfield data

The measurements were done at CAHA in coudé room in the T2.2 m building. A halogen lamp with a 10 W (Osram M326 6V 10W) light bulb was placed above the instrument entrance (Figure 1), and the H-bandpass filter in the beam. The lamp was fed with a stabilized power supply and a voltage of 0.95 V. In all the cases, the room was kept dark except for the lamp.
The calibration sequence was read with the cntsr-mode, as it is the mode recommended for PANIC since the other modes show a significant reset level drift. The data was saved as individual frames.

4 ANALYSIS

4.1 Data averaging

The analysis is based on CDS data. Therefore, the first frame (reset level) is subtracted from the last frame of each exposure. Figure 2 shows an example of the individual CDS values of a single pixel at the shortest integration time (2.9 s, first point of the ramp), which appear randomly distributed and without a significant drift.

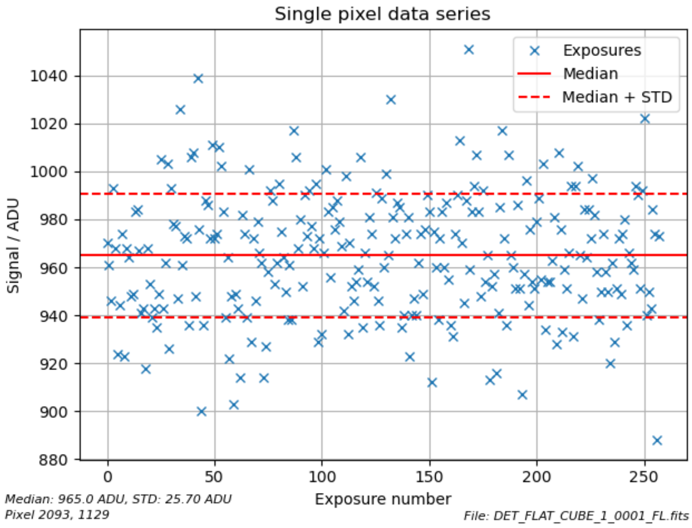

Figure 2: Single CDS data of one exemplary pixel with 2.9 s integration time (258 repetitions)

The CDS values are then median-averaged per pixel with 3-sigmal clipping and maximum 2 repetitions. Also, the standard deviation is calculated and saved. For the above example, with a median of 965 ADU and a standard deviation of 25.7 ADU, the error of the averaged value is then 1.6 ADU or 0.17%, as intended.

4.2 Offset subtraction

As described in RD 2, the reset value apparently changes between the first and second frame. The CDS data is therefore corrected with the reference CDS offset values per pixel.

4.3 Drift removal

4.3.1 Reference data fit

The reference exposures with constant exposure time throughout the measurement duration are averaged as described in Section 4.1. However, the CDS offset is not subtracted, as it was introduced later and the difference of about 30 ADU has no significant impact on the relative change between the exposures at about 12,500 ADU.

The median of the detector array—excluding a border of 50 pixels—is calculated per image. Each image is then scaled to the first one in the measurement procedure to obtain the relative change. The timestamps of the integration start and end per measurement are averaged to obtain the timestamp for each reference data point.

The time series is fitted with a 4th-order polynomial, and shown in Figure 3 left, and the residuals on the right. There is an apparent drift of the reference data of up to 1.2%, probably due to the light source, but also some random noise. The residuals are in the range of up to 0.3%. This is therefore the noise floor per point for the following analysis.

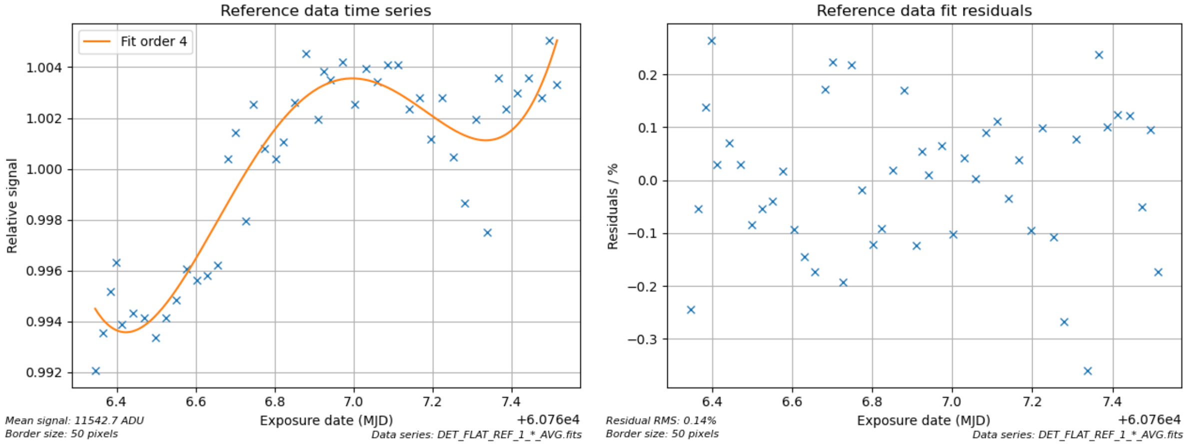

Figure 3: Left: Reference data time series of the calibration data, taken between each ramp image, and 4th-order polynomial fit. Right: Fit residuals

4.3.2 Drift correction

For each linearity ramp measurement, the average timestamp is calculated from the start and end of the integration. The image and standard deviation is then scaled with the inverse of the reference polynomial value obtained before. Note that no frame-based correction is done, as the random noise in the reference data is larger than the relative change on the timescale of individual images.

4.4 Linear extrapolation

4.4.1 Formula and evaluation

In an ideal detector, the signal S_t is a linear function of the exposure time t with offset 0. However, the measured signal S shows a non-linear behavior. This already starts at the very beginning of the integration. Nevertheless, a simple linear fit to the data points of the short integration times yields an intercept or $S_l(t = 0)$ far from 0.

A better way to estimate the true linear signal is to fit an exponential function similar to RD 3 of the form

$$S_e(t) = a + \alpha\left(\exp\left(\frac{t}{\beta}\right) - 1\right) \tag{2}$$

to data points with small values. Note that the deviation from linearity is positive, as the ramps show a positive curvature at small signals, and reverse direction around half maximum.

When expressing the true signal as

$$S_l(t) = a + bt \tag{3}$$

the parameter a can be taken from the fit of Equation (2), while its derivate at $t = 0$ gives the slope:

$$b = \frac{dS_e}{dt}\bigg|_{t=0} = \frac{\alpha}{\beta}$$

The exponential fit is created with the data from $t_i = 2.9 - 29\ s$ integration time, and with the fixed parameter $a = 0$, since the offset has been corrected.

Pixels are excluded and marked as non-correctable if the signal at $t_i = 29\ s$ is below 30% or above 120% of the respective median image value, which rejects those with low QE or high dark current.

An example of the exponential fit and the derived linear extrapolation is shown in Figure 4.

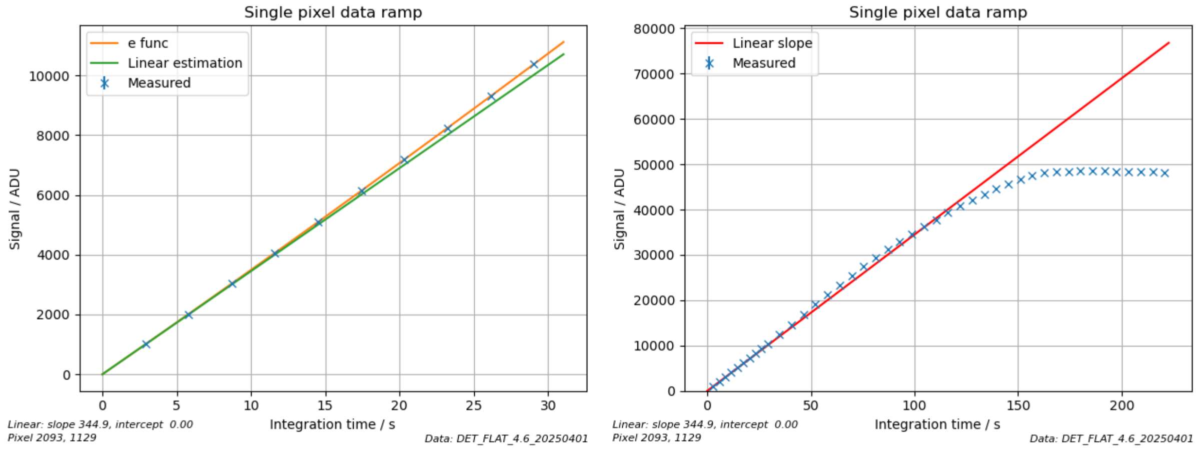

Figure 4: Left: Example of exponential fit to small data points and linear extrapolation showing the nonlinear behavior at low signal levels with an upward deviation. Right: Full ramp with linear slope, approaching saturation at about 48,000 ADU. Error bars per point are drawn but too small to be visible.

The intercepts are 0 by definition, since the data is reset-level and offset corrected. A fit without offset subtraction yields an almost identical linear slope (Figure 5 left), and intercept values close to the CDS reference offset within 5—10 ADU (Figure 5 right).

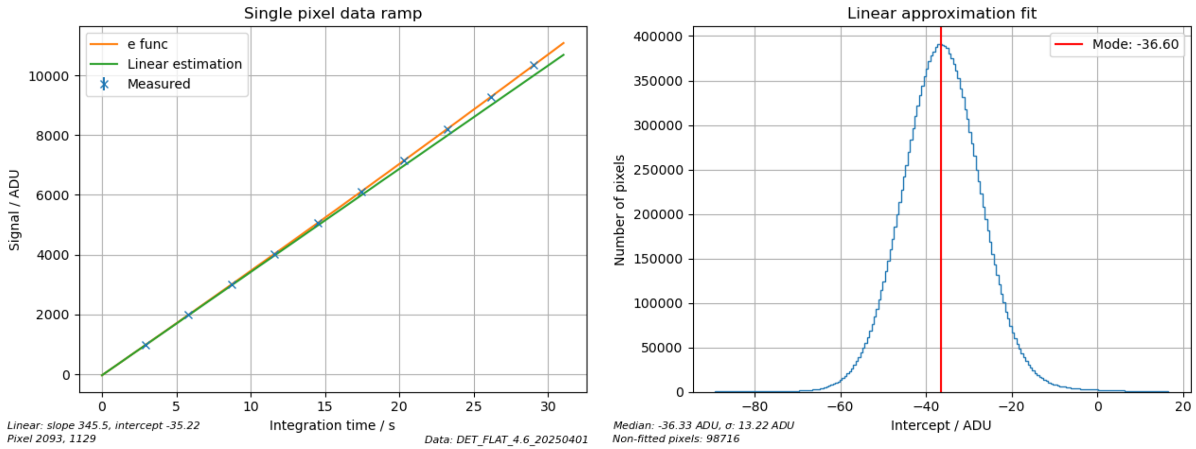

Figure 5: Left: Linear fit without offset subtraction but almost identical slope as above. Right: Histogram of linear slope intercepts for 0 integration time without offset subtraction.

It would also be possible to subtract the fitted offsets instead of the reference, however it turned out to yield more varying and noisy correction residuals. This is probably due to a still not precise extrapolation towards 0. The extrapolation of other datasets used in the verification in Chapter 5 lead to other offset medians and confirm the inaccurate determination via the fit.

The linear slopes are distributed as shown in Figure 6. The distribution is skewed due to an uneven flatfield illumination. As mentioned before, pixels below 30% of the median image (about 96 ADU/s) and above 120% (382 ADU/s) are excluded, which seem reasonable limits.

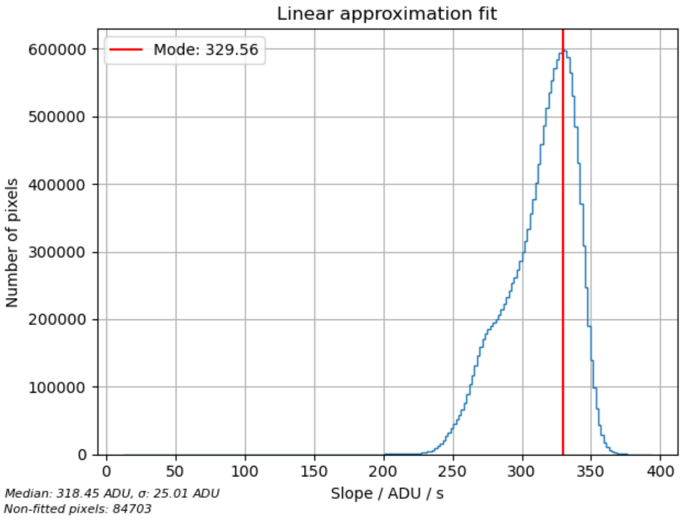

Figure 6: Histogram of linear slopes. The skewed distribution is caused by an uneven flatfield illumination.

4.4.2 Nonlinear behavior

To illustrate the nonlinear behavior on the full ramp, the relative residual to the linear extrapolation is calculated as $\Delta S_{rel}(t) = (S(t) - S_l(t))\ /\ S_l(t)$. For a single pixel it is shown in Figure 7 left, the median of all pixels in Figure 7 right. Apparently, the ramps are non-linear from the very beginning. The deviation is positive at first with measured signals higher than the linear ramp, at about half full well it changes curvature, and then levels out until saturation. The deviations are in the range of -15% to +6%.

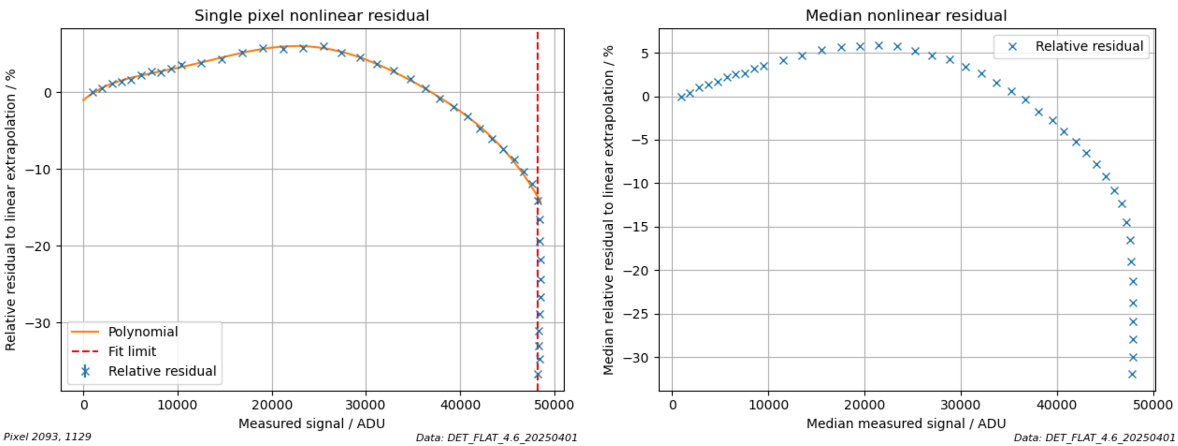

Figure 7: Left: Relative residual to linear extrapolation of a single pixel, already including the nonlinearity polynomial fitted in the following. Right: Median of all pixels

4.5 Polynomial fit

4.5.1 Principle

With the linear extrapolation (3), S_l is calculated for all exposure times t_i. The correction function of Equation (1) is the ratio between the linear and the measured signal:

$$P(S(t)) = \frac{S_l(t)}{S(t)} \tag{4}$$

It is fitted with a polynomial of 6th order with the coefficients $c_{1\dots7}$:

$$P(S(t)) = \sum_{j=0}^{6} c_{j+1}\, S(t)^j \tag{5}$$

This way, the optimization works with the relative residuals and not absolute ones, as it is the goal to minimize the relative error of the nonlinearity correction. When multiplying the polynomial again with the measured signal, effectively a polynomial of 7th order without constant term is obtained:

$$S_p(t) = P\big(S(t)\big) \cdot S(t) = \sum_{j=1}^{7} c_j\, S(t)^j \tag{6}$$

4.5.2 Fit process

The polynomial for each pixel is derived with the following optimizations:

If no linear fit is available, the pixels is skipped and marked as non-correctable.

The ramp initially contains N points. If the second to last signal is too high compared to the saturation value $S(t_{N-1}) > 0.99 \times S(t_{max})$, the ramp end is considered saturated and cannot be fitted. Therefore, the last point is excluded, and the ramp evaluated again with the remaining $N_{new} = N_{old} - 1$ points.

If the correction needed is larger than 25% for any of the points, i.e. $\left|\frac{S_l(t_i)}{S(t_i)} - 1\right| > 0.25$ for one $i = 1 \dots N$, the ramp is considered as non-correctable (highly nonlinear behavior or bad linear extrapolation). The last point is excluded and the ramp evaluated again with the remaining $N_{new} = N_{old} - 1$ points.

If at least 10 points are available ($N \geq 10$), the polynomial fit is done. To judge the fit quality, the relative residual is calculated for all integration times as $\Delta S_{rel}(t_i) = \frac{S_p(t_i) - S_l(t_i)}{S_l(t_i)}$. If the mean value of $\Delta S_{rel}(t_i)$ is < 0.002, and its standard deviation < 0.01, the fit is accepted. If the residual is larger, the last point is excluded and the ramp evaluated again with the remaining $N_{new} = N_{old} - 1$ points.

This is done until a sufficiently small residual is obtained, or the minimum number of points is reached. If no fit can be found, the pixel is marked non-correctable (unstable or noisy).

The outputs of the fitting are maps of polynomial coefficients c_j and a map of maximum correctable signal S_{max}. The maximum measured value used in the fit $S(t_N)$ is saved, and 98% of this value is set as the maximum correctable signal for this pixel S_{max}.

The polynomial coefficients c_{2-7} for all non-correctable pixels are set to 0, while $c_1 = 1$. To mark them as non-correctable, S_{max} is set to NaN.

4.6 Results

4.6.1 Polynomial fit quality

The polynomial of one example pixel on the relative deviation is shown above in Figure 7 left. It follows the data very well across the full range. Note that at 0 signal, the fit is typically <0 for the relative residual, meaning a correction >1.

The ramp data is shown in Figure 8. The left plot displays the linear signal vs. the measured signal. At the end, the pixel runs into saturation. To fit the polynomial, only points below the full well are used. Note that the saturation value decreases again with longer integration times, most likely caused by a rising reset value with higher signal in the detector, while the upper limit defined by the ADC remains constant.

The right plot shows the relative residuals for the measured data. Points where the saturation is reached are above the correction limit, and have a larger residual off the plot scale.

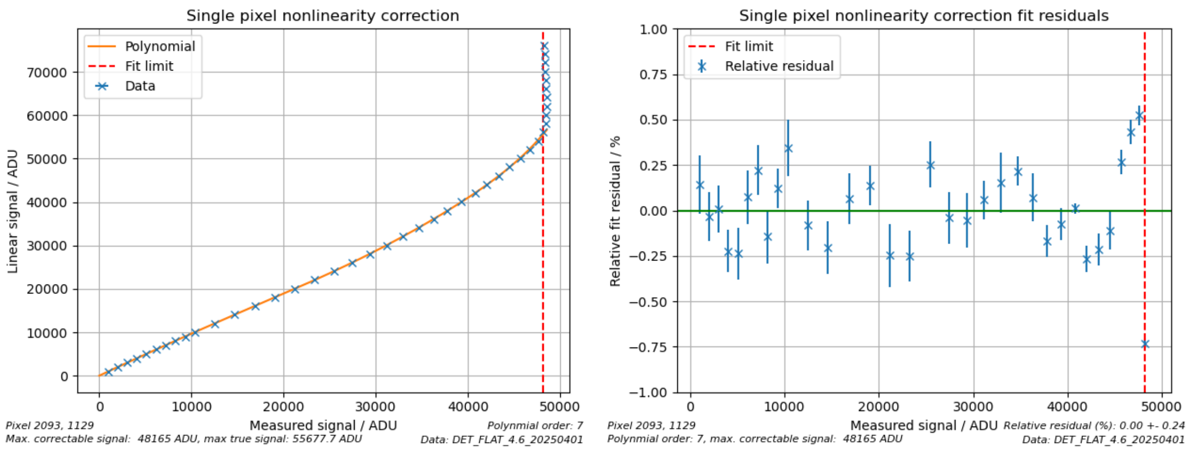

Figure 8: Left: Example of nonlinearity polynomial fit reaching close to saturation. Right: Relative residuals of the polynomial fit. The variation is of similar magnitude as the stability observed in the reference data, and no systematic pattern is present.

The fit works very well with a relative residual RMS of 0.24% for this pixel. The values are evenly distributed, and the magnitude is in the range of ±0.3%, which is similar to the accuracy limit determined by the reference data. No systematic pattern in the residuals is present beyond this limit. Also, no point-wise alternating pattern is visible, which would be caused by systematic errors on the ramp and the even-odd measurement sequence. Note that the last point here has the largest residual, and is excluded for the correction by setting the maximum correctable signal to 98% of the fit limit.

The histogram of the relative residual RMS is shown in Figure 9. Most of the ramps can be fitted with an RMS below 0.35%. The sharp cutoff at 1% is due to the selection criterion in the fit.

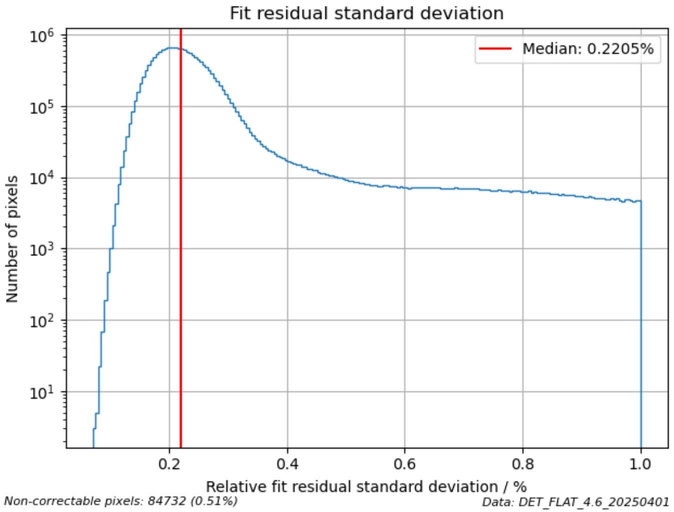

Figure 9: Histogram of relative fit residual RMS. For the majority of pixels it is <0.4%. The cutoff at 1% is due to the criterion for the fit quality.

4.6.2 Maximum correction limit

The maximum correction limit of all usable pixels is displayed in Figure 10. Most of them are usable up to their full well, a very small fraction has limits down to 5,000 ADU. Converted to electrons, the limits are in the range of 107 ke– (gain = 2.3 e-/ADU).

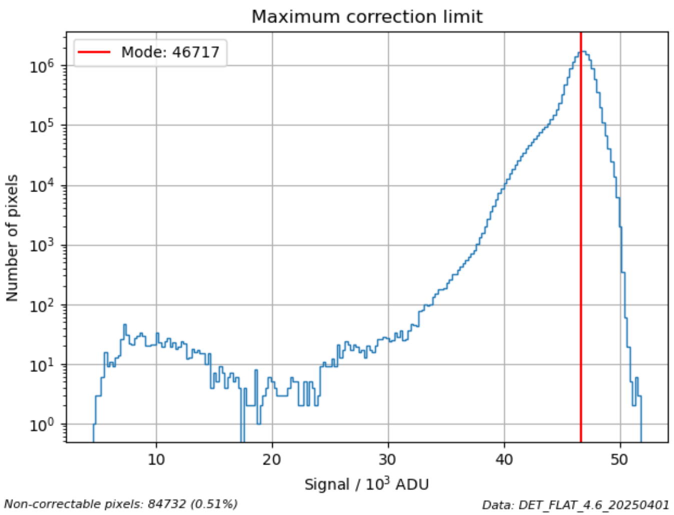

Figure 10: Histogram of maximum correctable signal in readmode cntsr. The mode value in ADU correspond to 107 ke–.

To better judge the usability of the fit, the histograms are once more created with the correction maximum relative to the full well (pixel value with the longest exposure time). As shown in Figure 11, 99.9% of the correctable pixels are usable up to 90% of their full well, and 99% up to 95%. The remaining ones apparently are not easy to fit with a polynomial, possibly caused by noisy outputs or high dark current.

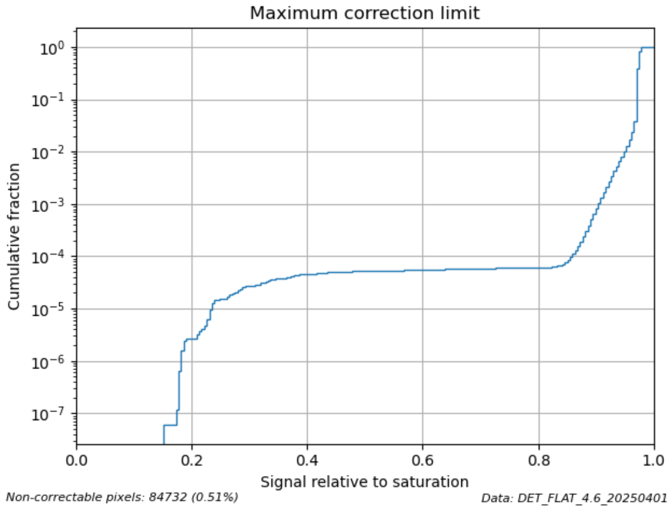

Figure 11: Cumulative histogram of relative maximum correction in cntsr mode.

The image of the maximum level is plotted in Figure 12. As expected, almost all pixels reach up to about 47,000 ADU. There is a pattern visible defined by the readout channels which points to a systematic reset level variation along the fast readout direction. The unusable pixels are mostly grouped in a scratch in the upper part, small local defects, the corners due to vignetting, and an electrically dead line.

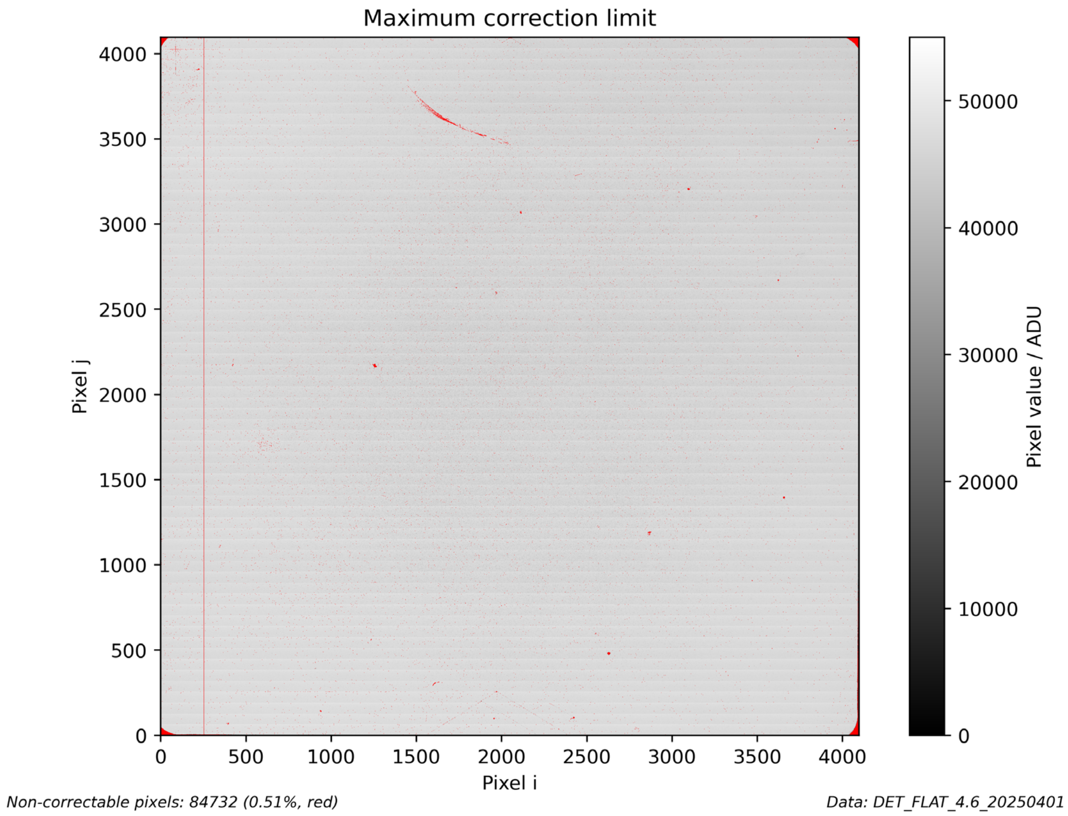

Figure 12: Image of the maximum correction in cntsr mode, linear scale 0–55,000 ADU. Non-correctable pixels are marked in red. 0.51% of the pixels could not be calibrated and are not usable. The pattern coincides with the readout channels, indicating a systematic reset variation along the lines.

To estimate maximum integration times, it is better to use the true maximum correctable signal, i.e., the linearity corrected value of the maximum data from above. The histogram is plotted in Figure 13. The maximum is around 53,000 ADU, converted to electrons around 121 ke– (Table 2).

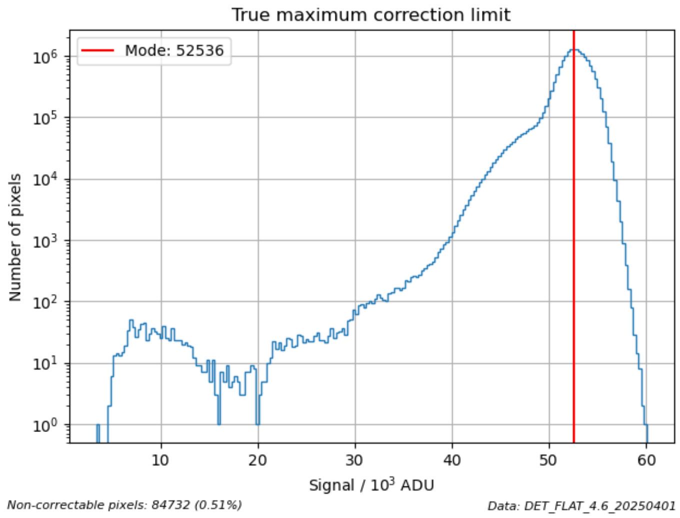

Figure 13: Linearity corrected usable limit cntsr mode. The mode value corresponds to 121 ke–.

Table 2: Usable range in cntsr mode: CDS counts, and linearized count numbers

		Usable range
Mode	ADU e–	46,717 107,449
Mode linearized	ADU e–	52,536 120,833

The number of non-correctable pixels is listed in Table 3.

Table 3: Amount of uncorrectable active pixels in cntsr mode

	Quantity
Number of uncorrectable active pixels	84732
Percentage of active pixels	0.51

Note that only 29 pixels more are excluded by the fit criteria compared to the selection in the linear extrapolation, meaning that the fit quality limit may reduce the maximum range, but hardly lead to exclusion of a pixel. The reduction of the maximum is however limited to a small fraction, as seen in the cumulative limit histogram.

4.6.3 Polynomial coefficients

The distribution of the polynomial coefficients is shown in Figure 14. The distributions have a well-defined maximum and a small asymmetry.

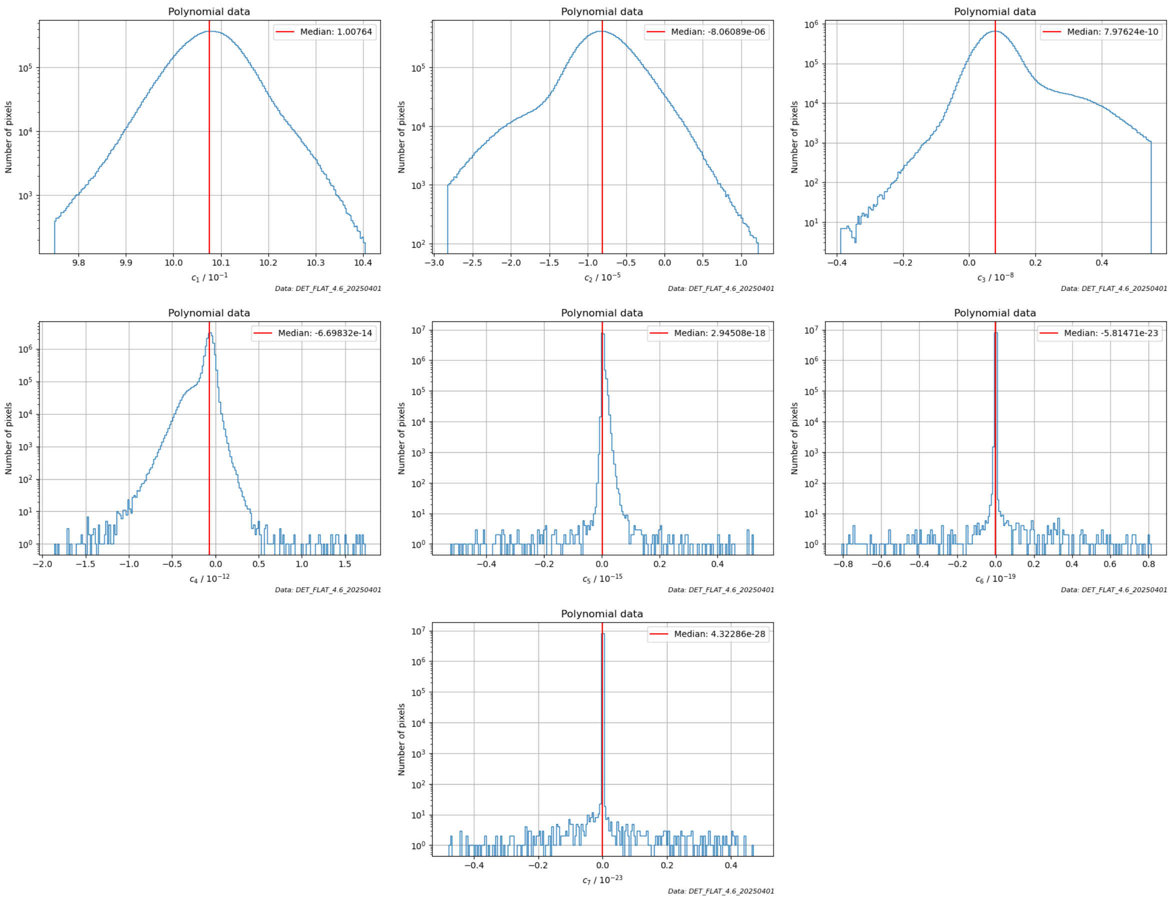

Figure 14: Polynomial coefficients c_1 (to top left) to c_7 (bottom) for read mode cntsr. The mode is marked with the red line.

4.7 Limitations

It is not possible to use calibration data that saturates in similar times as in operation. The shortest integration times resulted in too high signals and the ramp would contain too few points. The equivalence to higher irradiances has been verified in the following.

The most significant limitation is due to the measurement accuracy of 0.3%, possibly by light source effects. A mitigation could be to use a different filter with higher voltage on the lamp.

Of course, a new calibration always has to be created if the detector operation parameters are modified (timings, voltages).

5 VERIFICATION

5.1 Data

The correction data for this analysis is the file **`mNONLIN_CNTSR_01.01`** created in cycle 12. To demonstrate the application of the correction for different count rates, images were taken with different light levels with varying exposure times. The datasets are listed in Table 4. The calibration data has been analyzed as well. Note that newer correction data should not be used for exposures with other detector settings.

Table 4: Data for verification of nonlinearity correction with various saturation times

Cycle	Name	Vers.	Date	Content	GEIRS and pattern
12	DET_FLAT	4.0	23/11/2024	Series of flatfields, 90s sat. with H2 filter	r806M-154 (Nov 8 2024, 13:36:24)
12	DET_FLAT	4.3	03/12/2024	Series of flatfields, 160s sat. with H filter	r806M-154 (Nov 8 2024, 13:36:24)
12	DET_FLAT	4.4	28/02/2025	Series of flatfields, 20s sat. with H2 filter	r807M-76 (Feb 3 2025, 16:28:17)
	DET_FLAT	4.4	28/02/2025	Series of flatfields, 30s sat. with H filter	r807M-76 (Feb 3 2025, 16:28:17)
12	DET_FLAT	4.5	01/03/2025	Series of flatsfields, 160s sat. with H filter, up to 87s (60%)	r807M-76 (Feb 3 2025, 16:28:17)
12	DET_FLAT	4.6	01/04/2025	Series of flatfields, 160s sat. with H filter (calibration data)	r807M-76 (Feb 3 2025, 16:28:17)

5.2 Methods

The single exposures are processed as described in Sections 4.1, 4.2, and 4.3 (averaging, offset subtraction, drift correction). The nonlinearity correction as in Equation (6) is applied per pixel. Values that are above the maximum correction value are set to NaN, as well if that limit is NaN. A linear fit without offset is calculated with the valid data points by minimizing the relative residual RMS.
The correction quality is assessed by the relative residual to the linear fit per data point. The saturation fraction of the measured signal is calculated, and a 2D histogram is calculated over the saturation fractions and the relative residuals. For each saturation bin, the median value of the residuals is calculated.

5.3 Results

The signal ramps are presented for a random selection of ten pixels. In the plots, the measured data are crosses, the corrected ones the dots. The lines are the linear fit. Each ramp is offset by 3000 ADU from 0 to better distinguish between individual pixels, the nominal 0 is marked with a short line at the y-axis.
The residual histogram is displayed as an image in the range of ±10%, where each bin in the saturation direction (i.e. each histogram of residuals) is normalized to its maximum. The median value is plotted on top of the image, while the plot symbol size is scaled with the square root of the total number of points per bin to illustrate the amount of pixels.

5.3.1 Calibration data (160 s saturation)

The data was recorded with the procedure DET_FLAT 4.6 with the H-filter.

The plot in Figure 15 left shows the ramps. The ramps are almost perfectly straight. The varying saturation point is apparent due to small differences in efficiency or illumination.

The residual histogram prove the quality of the polynomial fit. The residuals are typically <0.5%. Towards saturation the residuals start to deviate a little, as it was apparent in the ramp fitting. However, also the number of pixels decreases, indicated by the smaller plot symbols.

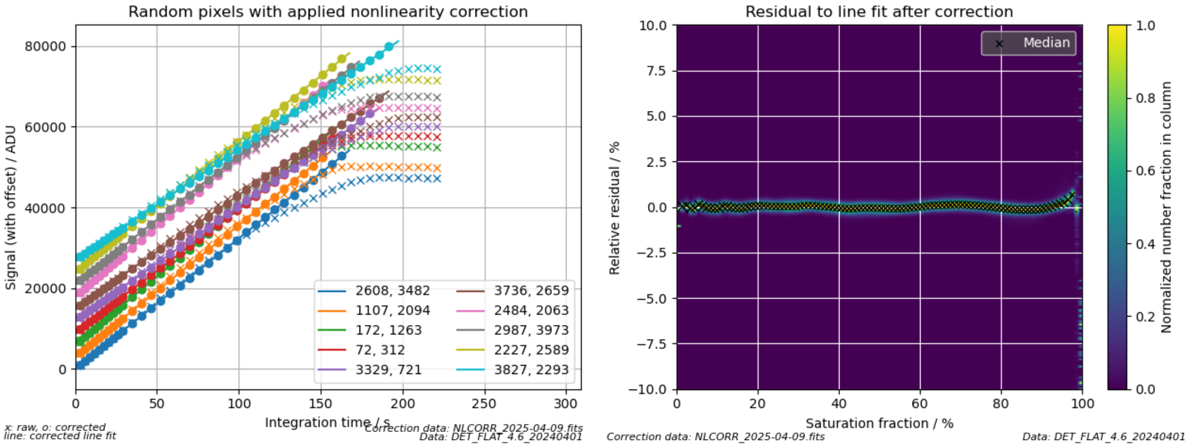

Figure 15: Calibration data (160 s saturation) from cycle 12. Left: 10 pixels ramps. Cross: measured, dots: corrected, line: linear fit. Right: Relative residual per saturation fraction, normalized per column, and median values, symbol sizes scaled with number of pixels.

5.3.2 Bright signals (20 s saturation)

The data was recorded with the procedure DET_FLAT 4.4 with the H2-filter.

The detectors will rarely be used with long integration times, in particular for stars. To check the correction with faster integrations, brighter sets were acquired, one of them with an approximate saturation of 20 s.

The ramps are shown in Figure 16 left. There are fewer points, and the lines are very well matching the data. The residual map on the right show deviations below 1% for most values. Towards smaller signals, the errors increase, probably due to an imperfect offset. However, the number of pixels decreases as well. The first ramp point at this illumination is typically above 10%, therefore data below results from otherwise problematic pixels, which should be filtered by noise or hot pixel selection. The effect is therefore not considered relevant.

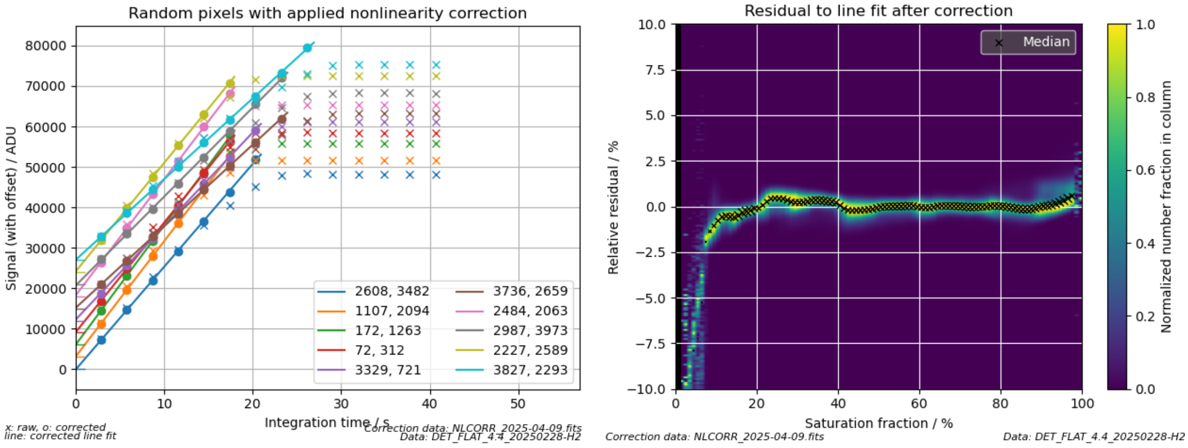

Figure 16: Data with 20 s saturation from cycle 12. Left: 10 pixels ramps. Cross: measured, dots: corrected, line: linear fit. Right: Relative residual per saturation fraction, normalized per column, and median values, symbol sizes scaled with number of pixels.

5.3.3 Bright signals (30 s saturation)

The data was recorded with the procedure DET_FLAT 4.4 with the H-filter.

The ramps are shown in Figure 17 left. The lines are very well matching the data. The residual map on the right show deviations below 1.2% for all values. Towards smaller signals, a systematic drop is visible, probably linked to the first ramp point, as well as a upward trend at the high end.

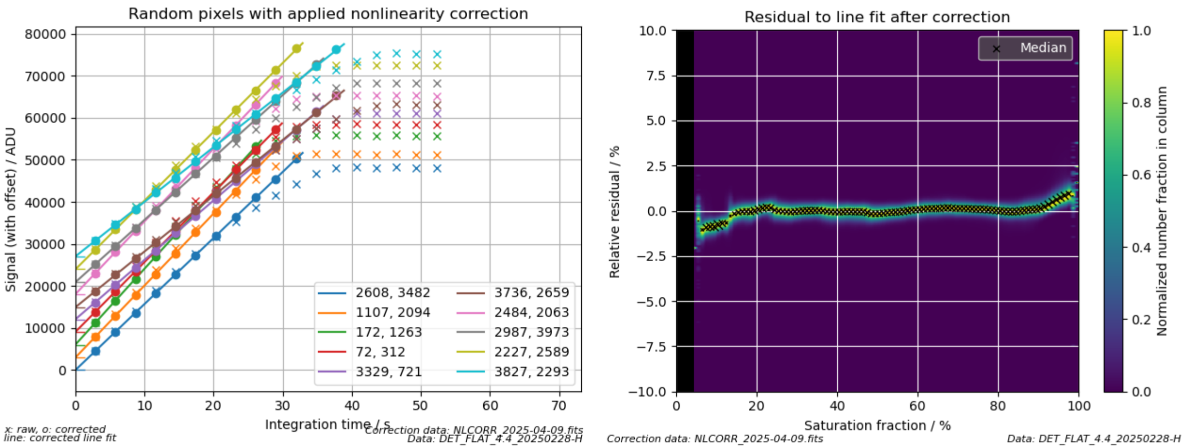

Figure 17: Data with 30 s saturation from cycle 12. Left: 10 pixels ramps. Cross: measured, dots: corrected, line: linear fit. Right: Relative residual per saturation fraction, normalized per column, and median values, symbol sizes scaled with number of pixels.

5.3.4 Medium signals (90 s saturation)

The data was recorded with the procedure DET_FLAT 4.0 with the H2-filter. The measurements were done with a constant number of 5 repetitions per integration time, so the noise on the fainter data increases compared to the optimized procedures.

The ramps are shown in Figure 18 left. The lines are very well matching the data. The residual map on the right show deviations up to 1.5% and a clear systematic shape. Towards smaller signals, the noise in the data becomes apparent. The errors increase as well, probably due to an imperfect offset.

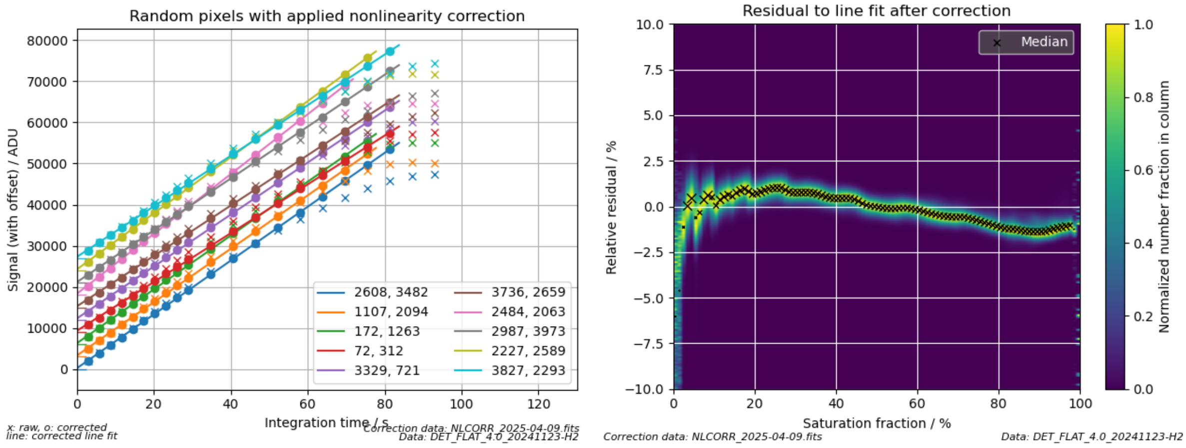

Figure 18: Data with 90 s saturation from cycle 12. Left: 10 pixels ramps. Cross: measured, dots: corrected, line: linear fit. Right: Relative residual per saturation fraction, normalized per column, and median values, symbol sizes scaled with number of pixels.

5.3.5 Faint signals (160 s saturation)

The data was recorded with the procedure DET_FLAT 4.3 with the H-filter. The measurements were done with a constant number of 10 repetitions per integration time, so the noise on the fainter data increases compared to the optimized procedures.

The ramps are shown in Figure 19 left. The lines are very well matching the data. The residual map on the right show deviations up to 1.2% and a clear systematic shape. Towards smaller signals, the noise in the data becomes apparent.

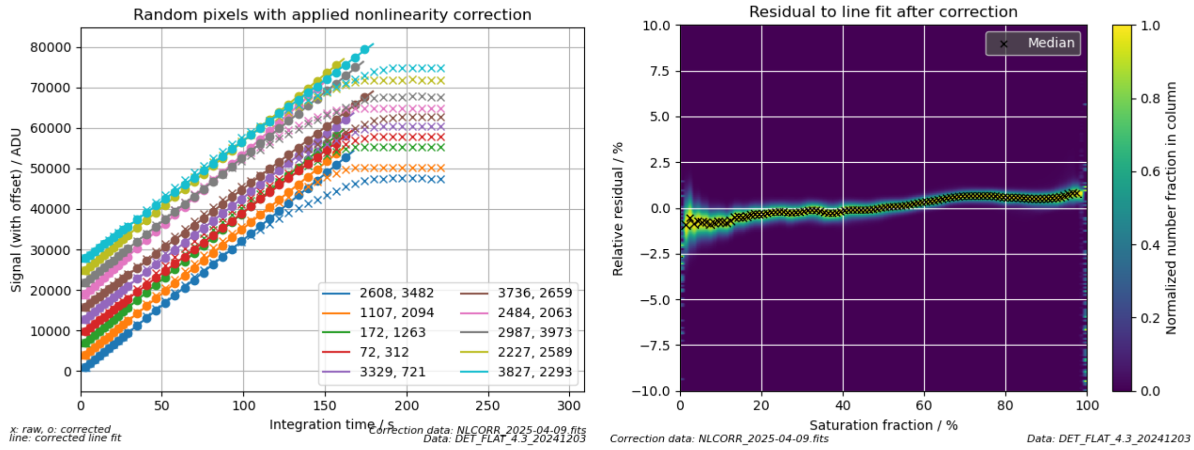

Figure 19: Data with 160 s saturation from cycle 12. Left: 10 pixels ramps. Cross: measured, dots: corrected, line: linear fit. Right: Relative residual per saturation fraction, normalized per column, and median values, symbol sizes scaled with number of pixels.

5.3.6 Faint signals (160 s saturation, short ramp)

The data was recorded with the procedure DET_FLAT 4.5 with the H-filter. The number of exposures was adapted to reduce the shot noise, but the ramp was only covered up to about 60% saturation.

The ramps are shown in Figure 20 left. The lines are very well matching the data. The residual map on the right show deviations below 0.3% up to the nominal signal level. The values above 60% saturation cannot originate from normal pixels and are not considered relevant.

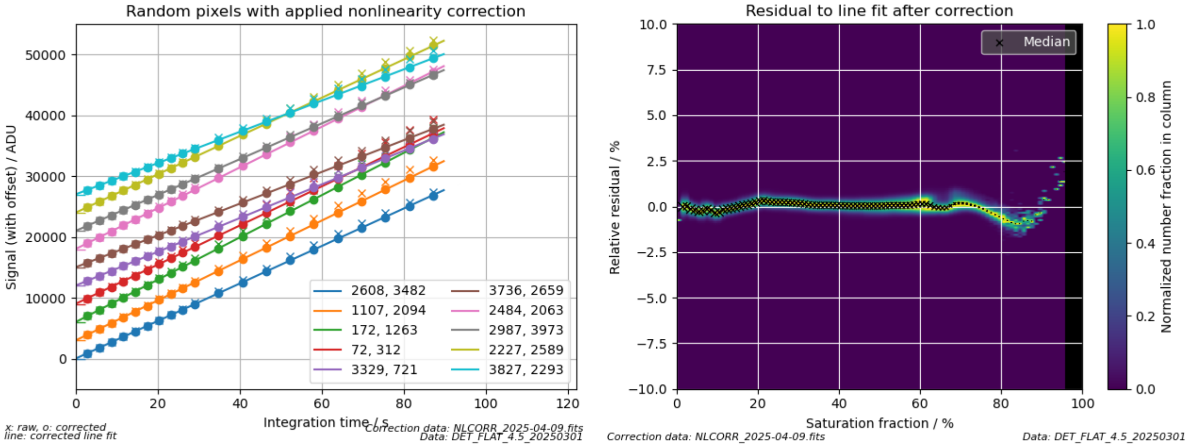

Figure 20: Data with 160 s saturation from cycle 12 up to 60%. Left: 10 pixels ramps. Cross: measured, dots: corrected, line: linear fit. Right: Relative residual per saturation fraction, normalized per column, and median values, symbol sizes scaled with number of pixels.

5.4 Conclusion

The verification demonstrates that the derived correction yields residuals below 0.5% for some measurements, while for others there are systematic errors up to 1.5% as in the 90 s-set. It does not appear to be filter dependent, since there is little difference between the 20 s and 30 s data, which were taken in the same measurement run with H2 and H filters. Besides, the 160 s-set also has a systematic error, while being recorded with the same filter as the calibration data. Notably the residual shape and direction of the larger deviations is different.

One common feature of these measurements is that they were recorded with a constant number of exposures per integration time, while the others have been adjusted to reach a total number of counts for constant shot noise. However, it is unlikely that this influences the ramp shape, as it should only increase the variation per saturation fraction, as apparent in the 160 s-data. Eventually, the origin for this systematics is unknown.

The uncertain offset leads to larger errors for small signals, but does not influence the overall ramp shape. In fact, analyses with subtraction of the fitted intercept of the exponential functions instead of the reference showed more noise on the residuals, while not changing the overall shape.

The observed larger residuals are linked to otherwise questionable pixels, which should be filtered by a proper bad pixel selection. Nevertheless, it indicates that the uncertain offset may still cause larger error for very small signals, if the reset change between first and second frame is not stable. To mitigate this, a better reset correction method has to be used.

Overall, the remaining error after nonlinearity correction is below 1.5% across the full range for nominal pixels.

6 REFERENCE FILES

6.1 File format

The fit results are stored in reference files in the FITS data format. The filename is composed as:
`mNONLIN_<readmode>_<version>.fits`
The valid strings are:

- `readmode`: GEIRS read mode in upper case, for now there is only "`CNTSR`".
- `version`: version and subversion as two-digit numbers 00-99 separated by a dot, e.g., "`01.03`".

The FITS file has a primary header with no data, and three data extensions for the detector array. They are labeled `LINMIN`, `LINMAX` and `LINPOLY`.
The extension `LINMIN` is a 32bit float 4096x4096 data array containing the lowest signal in the polynomial fit for each pixel. Uncorrectable pixels have a NaN instead of a numerical value.
The extension `LINMAX` is a 32bit float 4096x4096 data array containing the maximum correctable signal for each pixel. Uncorrectable pixels have a NaN instead of a numerical value.
The extension and `LINPOLY` is a 32bit float 4096x4096x7 data cube containing the polynomial coefficients $c_{1\ldots7}$ in reverse order. The first slice in the cube is c_7, the second c_6, etc.

6.2 Header data

6.2.1 Primary header

The primary header of the file contains data to identify the file type, characterization of the origin data, and parameters of the readout that influence the detector behavior. The entries are listed in Table 5.

Table 5: List of entries in the FITS primary header. The red marked ones can be used to check the applicability of a given file to an exposure.

Key	Value	Comment	Remarks
SIMPLE	T	conforms to FITS standard	Standard
BITPIX	0	number of array dimensions	Standard
NAXIS	0	number of array dimensions	Standard
EXTEND	T		Standard
ID	<filename>		Filename as described in 6.1
AUTHOR	<author name>		Name of creator
DESCR	<Data description>		Short description of file content
INSTRUME	'PANIC'		Instrument name

PAPITYPE	'MASTER_LINEARITY'	File data type as classified by the pipeline	Type of reference data
DATE	<ISO format date string>	UTC date of file creation	Timestamp of file creation
USE_AFT	<ISO format date string>	Use for data taken after this date	Day after which this data has to be used
DETROT90	<number>	[ct] 90 deg SW image rotations	GEIRS rotation value
DETXYFLI	<number>	[1] SW image flip (1=RightLeft, 2=UpDown, 3=bot	GEIRS data flip value
PREAD	<number>	[ns] pixel read selection	GEIRS readout parameter
PSKIP	<number>	[ns] pixel skip selection	GEIRS readout parameter
LSKIP	<number>	[ns] line skip selection	GEIRS readout parameter
READMODE	<read mode string>	read cycle-type	GEIRS readout parameter
IDLEMODE	<idle mode string>	idle to read transition	GEIRS readout parameter, see text
IDLETYPE	<idle type string>	idle cyle-type	GEIRS readout parameter, see text
B_EXT1	<number>	[V] external bias <digital value>	External bias voltage detector 1
B_DSUB1	<number>	[V] det. bias voltage DSUB <digital value>	DSUB voltage detector 1
B_VREST1	<number>	[V] det. bias voltage VRESET <digital value>	Reset voltage detector 1
B_VBIAG1	<number>	[V] det. bias voltage VBIASGATE <digital number>	Bias gate voltage detector 1
HISTORY	Description of creation		Comments on data origin and info
HISTORY	DOCUMENT:		
HISTORY	<Reference TN ID + version>		ID if the reference document + version number

HISTORY	SOFTWARE:		
HISTORY	<script name and version>		Filename of creation script and version
HISTORY	DATA:		Measurement procedure name
HISTORY	<GEIRS info string>		CREATOR entry in the exposure header
HISTORY	DIFFERENCES:		
HISTORY	<Version info>		Comment on differences to previous version

The data marked in light red should be checked and compared with the data of the exposure to correct, i.e., if the correction data is applicable to this file (instrument, `USE_AFT`) and if the data orientation and readout parameters are the same. The version of the readout pattern is only noted in the `HISTORY <GEIRS info string>`, as it may change without changing the timings and voltages. The values of `IDLEMODE` and `IDLETYPE` do not have to be checked. However, the correction is only valid for data that are read after reading at least one full image to assure the correct reset level. This can be achieved by using idlemode “wait” and idletype “ReadWoConv”, as described in RD 5. If any other mode or type is set, all data but the first read can be used and corrected the same way.

6.2.2 `LINMIN` extension

The header of the `LINMIN` extensions has the following keywords listed in Table 7.

Table 6: List of entries in the `LINMIN` extension header.

Key	Value	Comment	Remarks
XTENSION	‘IMAGE’	Image extension	Standard
BITPIX	-32	array data type	Standard
NAXIS	2	number of array dimensions	Standard
NAXIS1	2048		Standard
NAXIS2	2048		Standard
PCOUNT	0	number of parameters	Standard
GCOUNT	1	number of groups	Standard
EXTNAME	‘LINMAX’	extension name	Ext. name
BUNIT	‘ADU’		Unit of data
DESCR	'Min level for linearity correction'		Description of data

6.2.3 LINMAX extension

The header of the LINMAX extensions has the following keywords listed in Table 7.

Table 7: List of entries in the LINMAX extension header.

Key	Value	Comment	Remarks
XTENSION	‘IMAGE’	Image extension	Standard
BITPIX	-32	array data type	Standard
NAXIS	2	number of array dimensions	Standard
NAXIS1	2048		Standard
NAXIS2	2048		Standard
PCOUNT	0	number of parameters	Standard
GCOUNT	1	number of groups	Standard
EXTNAME	‘LINMAX’	extension name	Ext. name
BUNIT	‘ADU’		Unit of data
DESCR	'Max level for linearity correction'		Description of data

6.2.4 LINPOLY extension

The header of the LINPOLY extensions has the following keywords listed in Table 8.

Table 8: List of entries in the LINPOLY extension header.

Key	Value	Comment	Remarks
XTENSION	‘IMAGE’	Image extension	Standard
BITPIX	-32	array data type	Standard
NAXIS	3	number of array dimensions	Standard
NAXIS1	2048		Standard
NAXIS2	2048		Standard
NAXIS3	7		Standard
PCOUNT	0	number of parameters	Standard
GCOUNT	1	number of groups	Standard
EXTNAME	‘LINPOLY’	extension name	Ext. name
DESCR	‘Polynomial coefficients (highest first), no offset’		Description of data

------&&&&&& End of document &&&&&&------